Electronic Supplementary Information

Outer-Sphere Reductive Elimination as the Enantio-Determining Step in Ir^{III}/Ni^{II} Metallaphotoredox-Catalyzed α-(Hetero)aryl Amination: A DFT Study

Ya-Bin Jiang [1], Wei Guan[2], and Yu-Jie Liang[1, 2]**

[1]Precision Medicine Laboratory for Chronic Non-communicable Diseases of Shandong Province, Institute of Precision Medicine, Jining Medical University, Jining, Shandong 272067, People's Republic of China

[2] Institute of Functional Material Chemistry, Faculty of Chemistry, Northeast Normal University, Changchun 130024, People's Republic of China

Table of Contents

COMPUTATIONAL DETAILS

1. Correction of Translational Entropy in Solution

We evaluated the electronic energy (E_{sol}) with zero-point energy correction in solution. For each species, the E_{sol} is defined through equation (S1):

$$E_{\mathrm{sol}} = E_{sol}^{pot} + E_{gas}^{v_0} \tag{S1}$$

the E_{sol}^{pot} is the potential energy including non-electrostatic energy in solution and $E_{gas}^{v_0}$ delegates the zero-point vibrational energy in the gas phase. In a bimolecular process, such as the Ni(I) complex capture the α-amino radical, the entropy change which can decreases considerably must be taken into consideration. In such case, Gibbs energy (G_{sol}^{o}) need be computed as follows:

$$\begin{aligned} G_{sol}^{o} &= H_0 - T(S_{\mathrm{r}}^{o} + S_{\mathrm{v}}^{o} + S_{\mathrm{t}}^{o}) \\ &= E^{T} + P\Delta V - T(S_{\mathrm{r}}^{o} + S_{\mathrm{v}}^{o} + S_{\mathrm{t}}^{o}) \\ &= E_{sol} + E_{therm} - T(S_{\mathrm{r}}^{o} + S_{\mathrm{v}}^{o} + S_{\mathrm{t}}^{o}) \end{aligned} \tag{S2}$$

where ΔV is 0 in solution, E_{therm} is the thermal correction by translational, vibrational, and rotational movements, and S_{r}^{o}, S_{v}^{o}, and S_{t}^{o} are rotational, vibrational, and translational entropies, respectively. In general, the Sackur-Tetrode equation is used to evaluate translational entropy S_{t}^{o}. In solution, however, the usual Sackur-Tetrode equation cannot be directly applied to the evaluation of S_{t}^{o}, because the translation movement is suppressed very much in solution.[S1] In this context, the translational entropy was corrected with the method developed by Whitesides et al., where the rotational entropy was evaluated in a normal manner. Thermal correction and entropy contributions of vibration movements to the Gibbs energy were evaluated with the frequencies calculated at 298.15 K and 1 atm.

2. Redox potential

We calculated the standard redox potential ($E_{1/2}^{red}$) according to the equation (S3):[S2]

$$E_{1/2}^{red} = -\frac{\Delta G_r}{nF} - E_{SCE} \quad \text{(S3)}$$

where, F is the Faraday constant and n is the number of electrons transferred, E_{SCE} = 4.51V, and ΔG_r is the free energy change of the reaction.

Table S1 The calculated redox potential of Ir complexes.

Redox Potential	Cal. i-PrOAc
$\mathbf{E_{1/2}^{red}}$ **[Ir^{IV}/*Ir^{III}]**	–1.48 V
$\mathbf{E_{1/2}^{red}}$ **[Ir^{IV}/Ir^{III}]**	1.26 V
$\mathbf{E_{1/2}^{red}}$ **[*Ir^{III}/Ir^{II}]**	1.13 V
$\mathbf{E_{1/2}^{red}}$ **[Ir^{III}/Ir^{II}]**	–1.81 V

Table S2 The calculated redox potential of Ni complexes.

Redox Potential	Cal. i-PrOAc
$\mathbf{E_{1/2}^{red}}$ **[Ni^{II}/Ni^{I}]**	0.13 V

Table S3 The calculated redox potential of **S1** complexes.

Redox Potential	Cal. i-PrOAc
$\mathbf{E_{1/2}^{red}}$ **[$S1^{+}$/S1]**	–1.58 V

Scheme S1. Single electron transfer processes. $\Delta G^{\circ\ddagger}$ values of SET processes are given in kcal/mol.

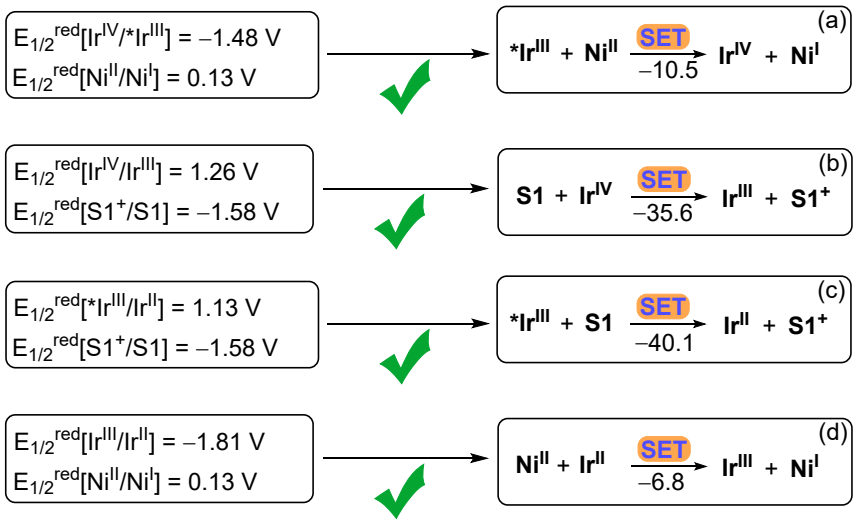

3. Activation barrier of single electron transfer step

According to the Marcus equation, the reorganization energy λ is normally decomposed into internal energy (λ_i) and external energy (λ_o). The internal reorganization energy λ_i can be estimated according to the equation:

$$\lambda_{i1} = [E^D(Q_R) + E^A(Q_R)] - [E^D(Q_P) + E^A(Q_P)] \quad \text{(S4)}$$

$$\lambda_{i2} = [\mathrm{E}^{\mathrm{D}^+}(\mathrm{Q_R}) + \mathrm{E}^{\mathrm{A}^-}(\mathrm{Q_R})] - [\mathrm{E}^{\mathrm{D}^+}(\mathrm{Q_P}) + \mathrm{E}^{\mathrm{A}^-}(\mathrm{Q_P})] \quad \text{(S5)}$$

$$\lambda_i = (\lambda_{i1} + \lambda_{i2})/2 \quad \text{(S6)}$$

where Q_R and Q_P are the equilibrium geometries of the reactants and products, respectively. In addition, the external reorganization energy λ_o may be calculated from equation (S7−S9)

$$\lambda_o = (332\ \text{kcal/mol})\left(\frac{1}{2a_1} + \frac{1}{2a_2} - \frac{1}{\mathrm{R}}\right)\left(\frac{1}{\varepsilon_{op}} - \frac{1}{\varepsilon}\right) \quad \text{(S7)}$$

$$\lambda = \lambda_o + \lambda_i \quad \text{(S8)}$$

$$\Delta G^{\circ\neq} = \frac{(\Delta G_r + \lambda)^2}{4\lambda} \quad \text{(S9)}$$

where a_1 is the radii of the oxidant, a_2 is the radii of the reductant, R = a_1 + a_2, ε_{op} is

the optical dielectric constant (ε_{op} = 2.25), ε is the static dielectric constant for the isopropyl acetate solvent (ε = 4.9), and ΔG_r is the free energy change of the reaction.

Table S4 Estimation of the activation barriers for SET step.

SET step	a_1 (Å)	a_2 (Å)	**R** (Å)	**λ** (kcal/mol)	**ΔG_r** (kcal/mol)	**ΔG_{SET}** (kcal/mol)
(a)	4.50	4.73	9.23	23.0	–10.5	1.7
(b)	3.46	4.59	8.05	32.4	–35.6	0.3
(c)	3.46	4.50	7.96	51.7	–40.1	0.7
(d)	4.73	4.31	9.04	23.9	–6.8	3.1

Table S5 The NBO population of key compounds.

species	Ir(III)	*Ir(III)	Ir(IV)	Ni(II) ^{T}**6**	Ni(I) ^{D}**1**	Ni(II) ^{T}**4**^{R}	Ni(III) ^{D}**3**	Ni(II) ^{T}**5**^{R}
Natural Charge of metal center	0.26	0.32	0.40	0.76	0.45	0.76	0.91	0.72
d-orbital population	7.83	7.75	7.66	8.33	8.87	8.39	7.50	8.34

Scheme S2. The sketch map of optical physical processes of **Ir^{III}**.

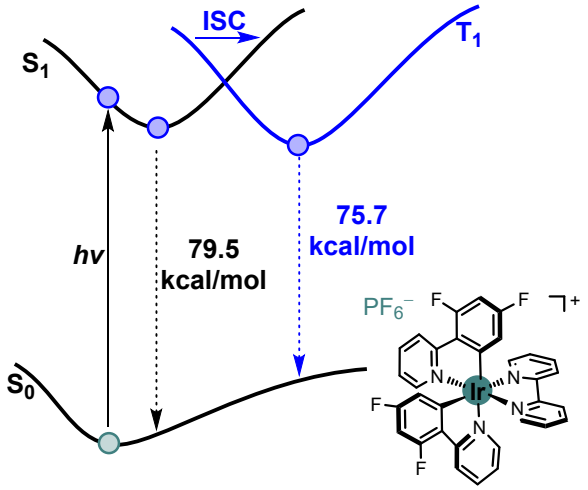

Scheme S3. The Gibbs free energy change ($\Delta G°_{298.15}$ in kcal/mol) of the reductive quenching process of ***Ir^{III}(Cl)** with ^{T}**Ni^{II}** to afford **Ir^{II}** and ^{D}**Ni^{III}** species steps for generating α-carbon centered radical.

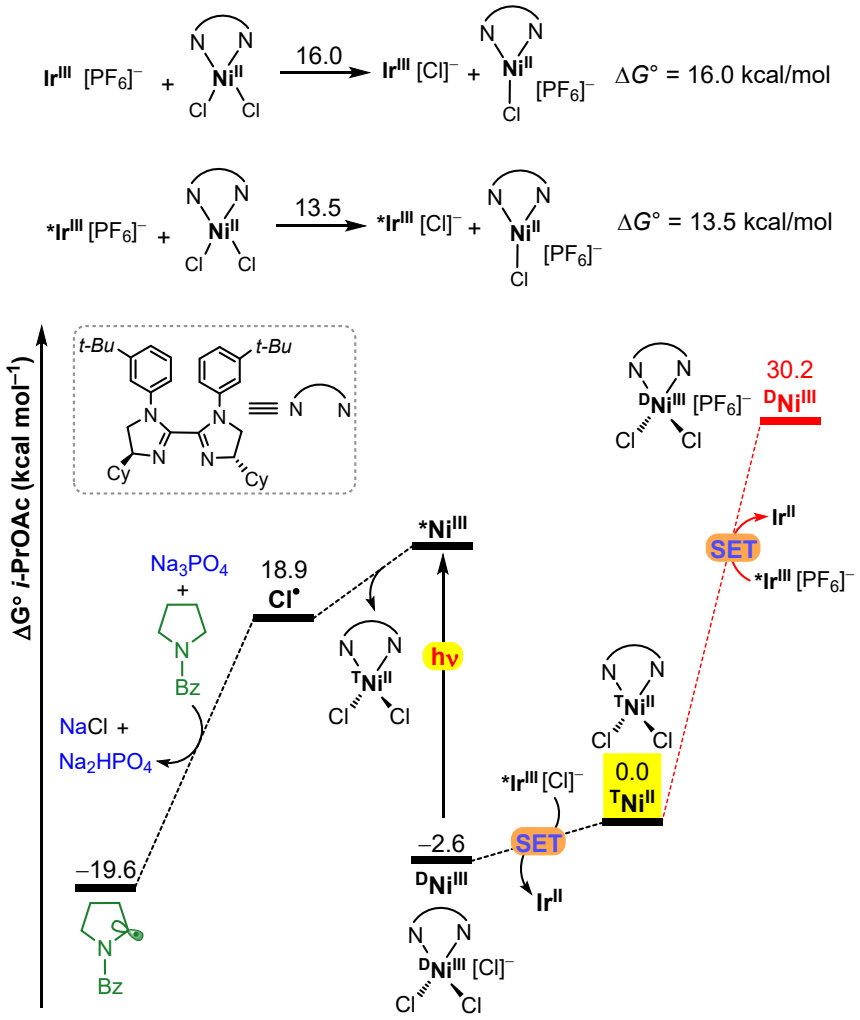

Scheme S4. Ir^{III}/Ni^{II} metallaphotoredox dual catalytic cycles: (A) (a1) oxidative quenching cycle of photocatalyst ***Ir^{III}** $[PF_6]^-$, (a2) reductive quenching cycle of photocatalyst ***Ir^{III}** $[PF_6]^-$, and (b) possible nickel catalytic cycles. (B) possible mechanism of photocatalyst ***Ir^{III}** $[Cl]^-$ participation.

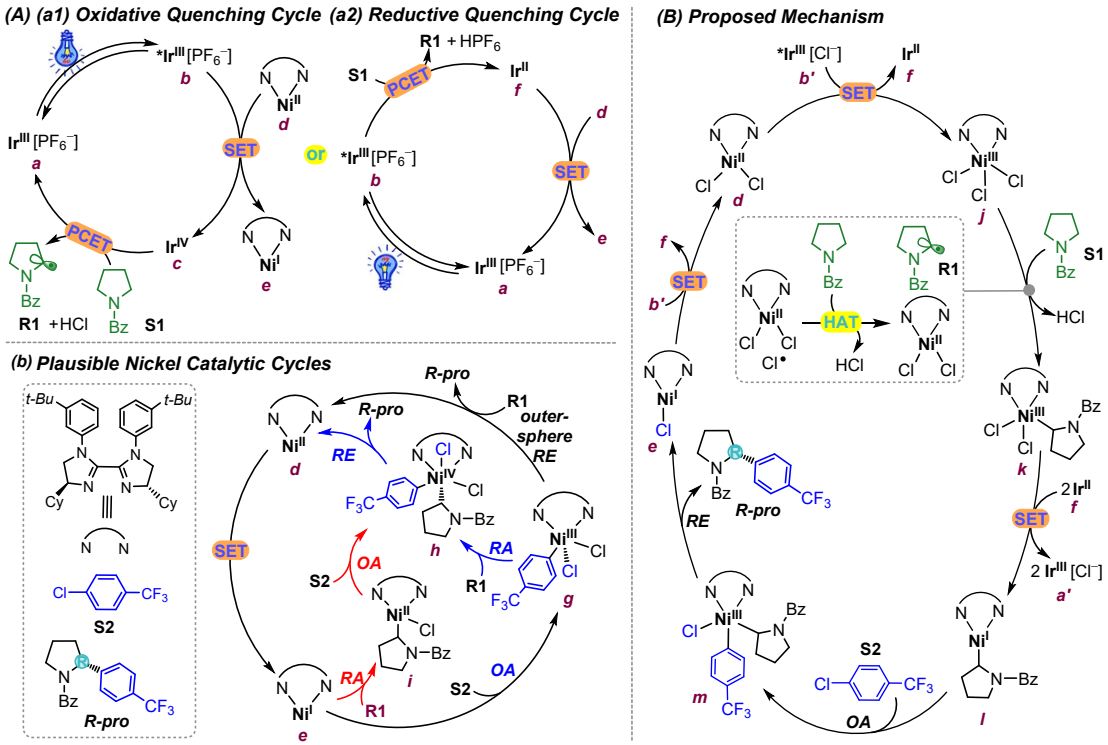

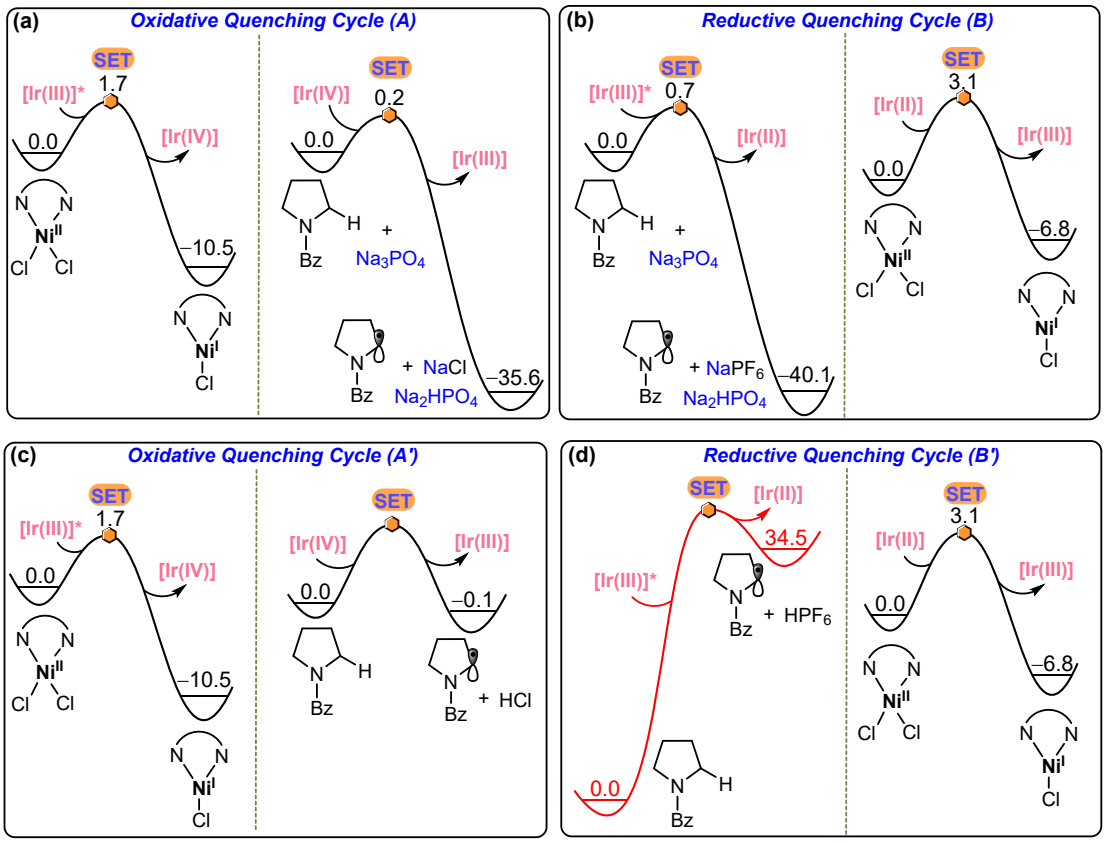

Fig. S1. Energy profiles ($\Delta G°_{298.15}$) of SET processes involved in the oxidative quenching and reductive quenching cycles in the presence (**a** and **b**) and absence of Na_3PO_4 (**c** and **d**).

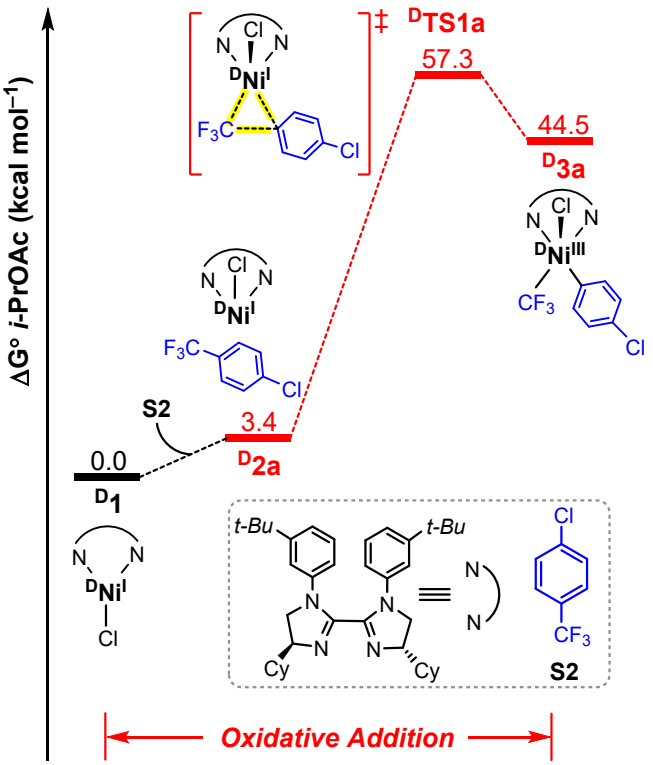

Fig. S2. Gibbs energy profile ($\Delta G°_{298.15}$) of C–CF_3 oxidative addition of **S2** to nickel(I) center in ^{D}**1**.

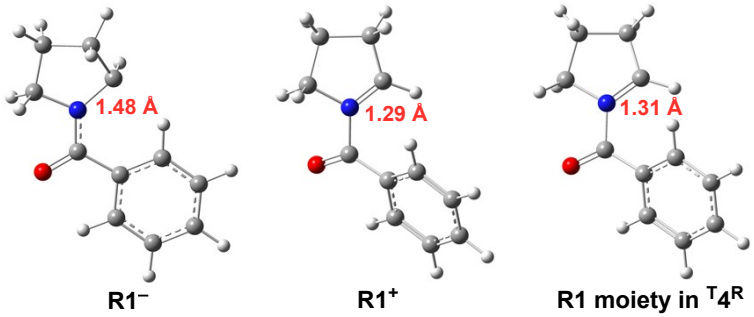

Fig. S3. Comparison of optimized geometries of anionic **R1**$^{-}$ and cationic **R1**$^{+}$ with **R1** moiety in ^{T}**4**^{R}.

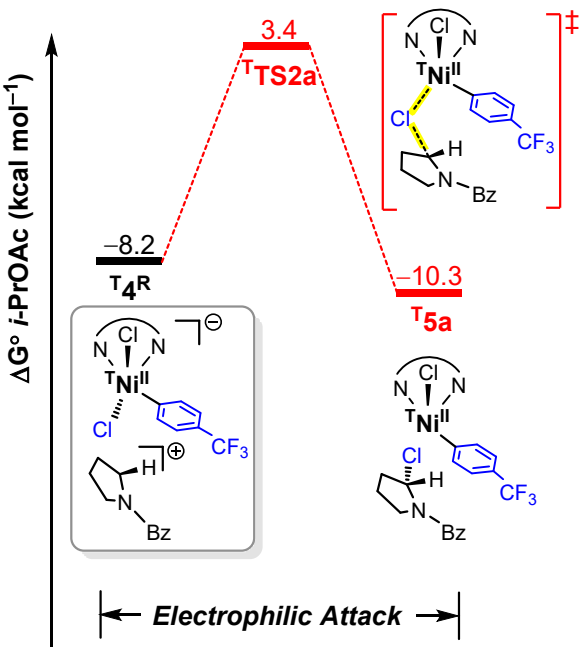

Fig. S4. Gibbs energy profile ($\Delta G°_{298.15}$) of the electrophilic attack to forge C–Cl bond.

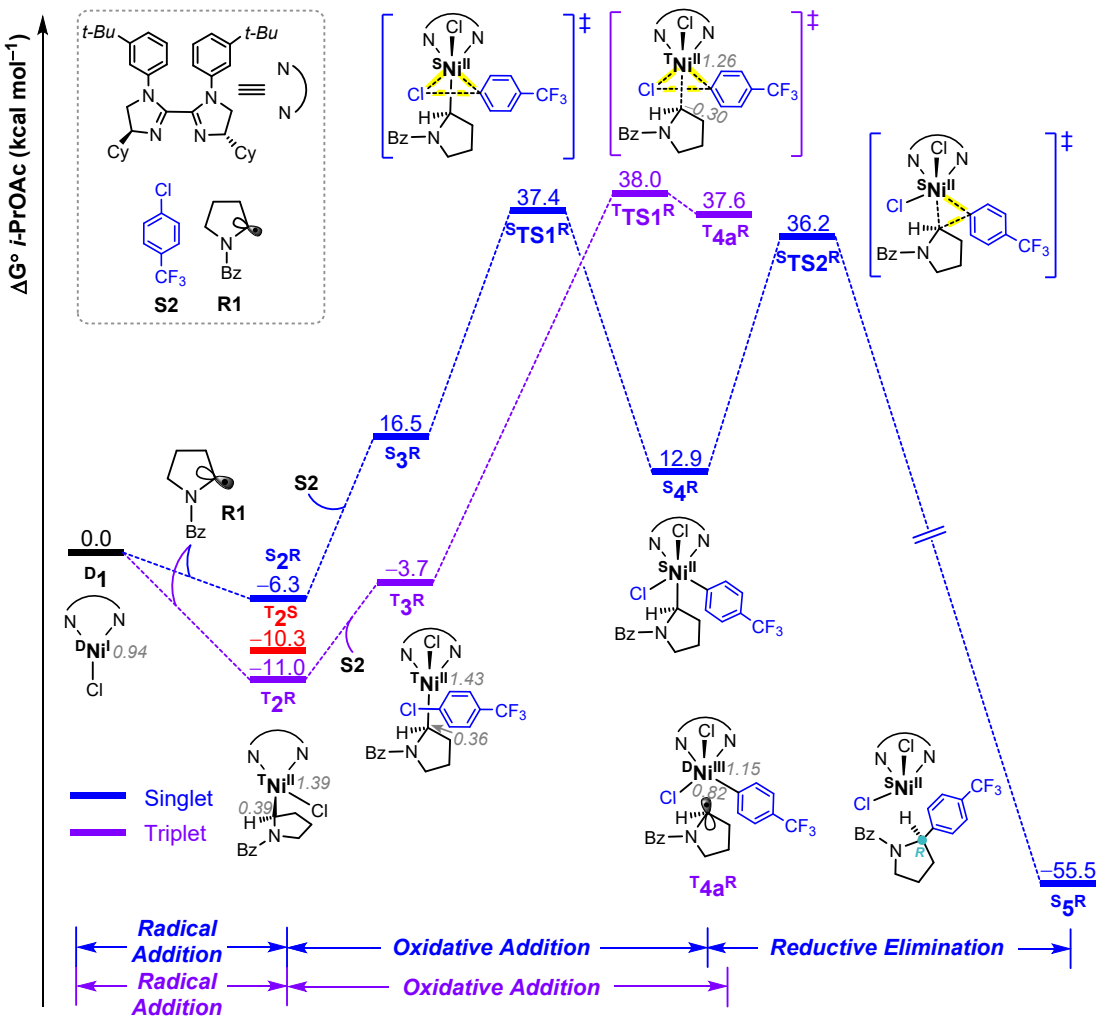

Fig. S5. Energy profiles ($\Delta G°_{298.15}$) of various competitive nickel catalytic pathways.

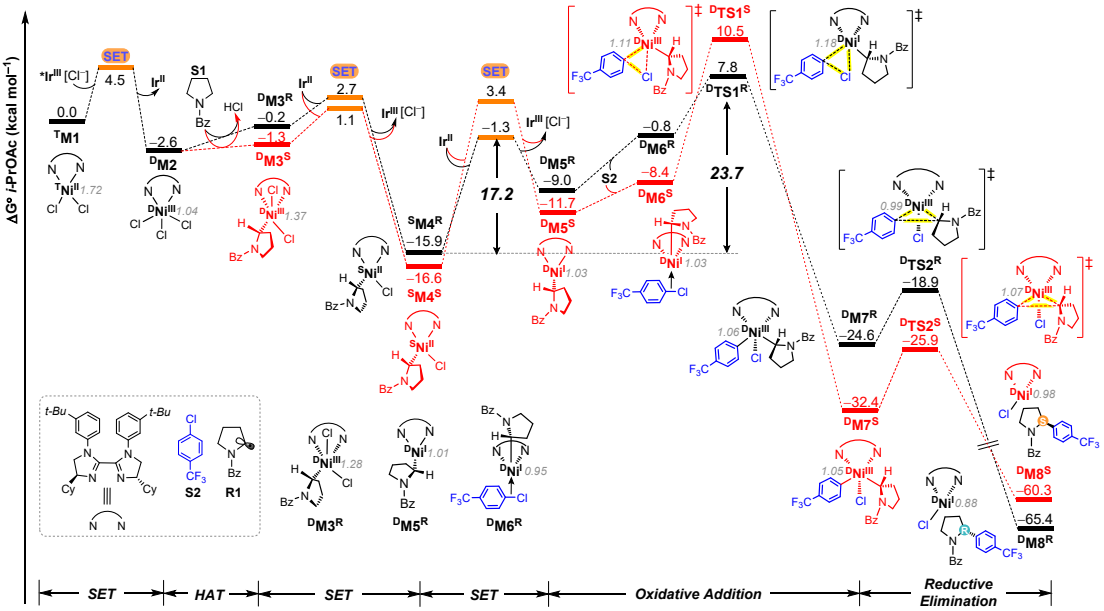

Fig. S6. Energy profiles ($\Delta G^{\circ}_{298.15}$) of various competitive nickel catalytic pathways (Scheme S3B).

In addition, we also considered the catalytic mechanism triggered by the photocatalyst Ir^{III}(Cl) in **Scheme S3B**. The results show that continuous single electron transfer is unfavorable with thermodynamically and kinetically ($^{D}M3^{R}$ → $^{D}M4^{R}$ → $^{D}M5^{R}$, $^{D}M3^{S}$ → $^{D}M4^{S}$ → $^{D}M5^{S}$). And this pathway in Fig. S6 has less favorable in reaction kinetics than Fig. 2 (23.7 kcal mol^{-1} *vs* 21.4 kcal mol^{-1}).

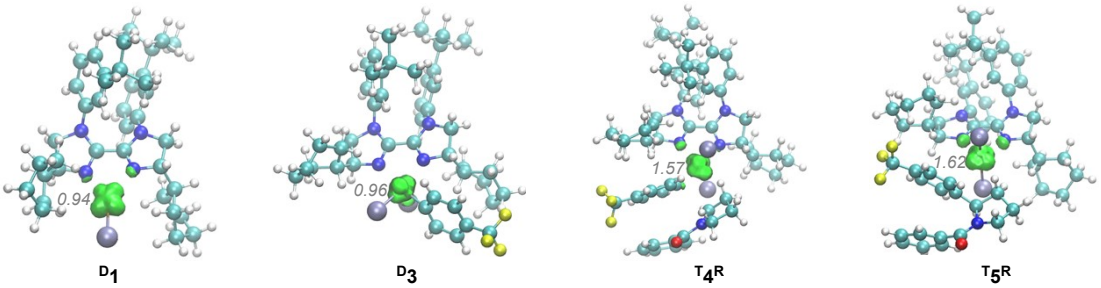

Fig. S7. Electron spin density of nickel compounds in various valence states (^{D}**1**, ^{D}**3**, ^{T}**4**^{R}, ^{T}**5**^{R}).

REFERENCES

S1. (a) Sakaki, S.; Ohnishi, Y. Y.; Sato, H., Theoretical and Computational Studies of Organometallic Reactions: Successful or Not? *Chem. Rec.* **2010**, *10*, 29–45; (b) Ishikawa, A., Nakao, Y., Sato, H.; Sakaki, S., Oxygen Atom Transfer Reactions of Iridium and Osmium Complexes: Theoretical Study of Characteristic Features and Significantly Large Differences between These Two Complexes. *Inorg. Chem.* **2009**, *48*, 8154–8163; (c) Ishikawa, A., Nakao, Y., Sato, H.; Sakaki, S., Pd(II)-Promoted Direct Cross-Coupling Reaction of Arenes via Highly Regioselective Aromatic C–H Activation: A Theoretical Study. *Dalton Trans.* **2010**, *39*, 3279–3289.

S2. Marenich, A. V., Ho, J., Coote, M. L., Cramer, C. J.; Truhlar, D. G., Computational Electrochemistry: Prediction of Liquid-phase Reduction Potentials. *Phys. Chem. Chem. Phys.* **2014**, *16*, 15068–15106.

S3. (a) Baba, H., Suzuki, S.; Takemura, T., Configuration Analysis in the LCAO Molecular Orbital Theory. *J. Chem. Phys.* **1969**, *50*, 2078−2086. (b) Kato, S., Yamabe, S.; Fukui, K., Molecular Orbital Calculations of the Electronic Structure of Borazane. *J. Chem. Phys.* **1974**, *60*, 572−578. (c) Dapprich, S.; Frenking, G., Rotational Analysis of n=4–7 Rydberg States of CO Observed by Ion-Dip Spectroscopy. *J. Phys. Chem.* **1995**, *99*, 9352−9362.